Pure appl. geophys. 158 (2001) 1583–1611
0033–4553/01/101583–29 $ 1.50 + 0.20/0

Pure and Applied Geophysics

Stable Continental Region Earthquakes in South China

LANBO LIU[1]

Abstract — This paper reviews some remarkable characteristics of earthquakes in a Stable Continental Region (SCR) of the South China Block (SCB). The kernel of the SCB is the Yangtze platform solidified in late Proterozoic time, with continental growth to the southeast by a series of fold belts in Paleozoic time. The facts that the deviatoric stress is low, the orientations of the major tectonic features in the SCB are substantially normal to the maximum horizontal principal stress, and a relatively uniform crust, seem to be the major reasons for lack of significant seismicity in most regions of the SCB. Earthquakes in this region are mainly associated with three seismic zones: (1) the Southeast China Coast seismic zone related to Guangdong-Fujian coastal folding belt (associated with Eurasia-Philippine Sea plate collision); (2) the Southern Yellow Sea seismic zone associated with continental shelf rifts and basins; and (3) the Downstream Yangtze River seismic zone spatially coinciding with Tertiary rifts and basin development. All three seismic zones are close to one or two major economic and population centers in the SCB so that they pose significant seismic hazards. Earthquake focal mechanisms in the SCB are consistent with strike-slip to normal faulting stress regimes. Because of the global and national economic significance of the SCB and its dense population, the seismic hazard of the region is of outstanding importance. Comparing the SCB with another less developed region, a pending earthquake with the same size and tectonic setting would cause substantially more severe social and economic losses in the SCB. This paper also compiles an inventory of historic moderate to great earthquakes in the SCB; most of the data are not widely available in English literature.

Key words: Stable continental region, South China block, tectonic stress, historic earthquakes, earthquake focal mechanism, seismic hazard.

1. Introduction

All major features of neo-tectonics and modern seismicity in continental China are controlled essentially by the collision between the India–Australian plate and the Eurasian plate along the Himalayan orogenic belt. In general, western China is tectonically and seismically more active than its eastern China counterpart. Nevertheless, part of eastern China has also experienced high seismicity, and sometimes, great earthquakes, although with a longer recurrence period. Moreover, the seismicity and tectonic evolution of the northern and southern parts of eastern China are quite different. The northeastern China region, part of the Sino–Korean

[1] Department of Geology and Geophysics, University of Connecticut, Storrs, Connecticut 06269-2045, USA. E-mail: Lliu@uconnvm.uconn.edu

platform, is undergoing extensional tectonic activities (e.g., the Shanxi graben and the Gulf of Bohai), and is characterized by a moderate to high seismicity. In contrast, the southeastern China region is characterized by much less seismicity and is more stable tectonically. The loosely defined southeastern China region will be the major part of the more specifically defined South China Block (SCB), which takes place in the next section. No major post Paleozoic tectonic activity has been identified in the SCB. Thus the SCB is one of the stable continental regions (SCR, JOHNSTON and KANTER, 1990; JOHNSTON, 1996a). Although the seismicity is low, study of earthquakes in this region is very important for two reasons. First, the Southeast China Coast seismic zone in the SCB coincides with one of the most developed economic zones in the entire China continent. Any moderate earthquake in this region may cause severe economic losses. Second, the population density in the SCB is one of the highest in Eurasia. Any destructive earthquake in the SCB could result in many more casualties than in the less populated western part of China. Since the economic reform started in the early 1980s, the coastal cities and regions in the SCB have been the most rapidly developing part of China and even of the entire Eurasian continent. The five economic zones in Guangdong and Fujian provinces (Shenzhen, Hainan, Shantou, Xiamen, and Zhuhai) are the best economic performers in China (e.g., STATE STATISTICAL BUREAU OF CHINA, 1999). For example, in 1996 the combined import/export volume for these five zones was \$59.1 billion, about 20% of the volume for all of China. The combined total gross production was over \$26 billion, a 14% growth of 1995. Meanwhile, the combined foreign investment in the SCB was \$3 billion, about 14% of total foreign investments in China (STATE STATISTICAL BUREAU OF CHINA, 1999). The population distribution shows that about 0.5 billion people live in the SCB. In Guangdong Province, the average number of people per square kilometer is well over 100. If a moderate earthquake occurs there and results in a 1000 square kilometers Intensity VI area of the Modified Mercalli Intensity (MMI) scale, it will greatly impact a minimum of 100,000 people. The seismic hazard in the SCB is further augmented by low attenuation of seismic waves in the SCR (e.g., NUTTLI, 1973; MITCHELL *et al.*, 1993). Thus a vastly larger region would be affected in the SCB than along plate boundaries for a similar size earthquake.

This paper discusses the tectonic background, seismicity and seismic hazards in the SCB. The definition of the SCB will be discussed in detail in the following sections. The SCB is the major part of the stable continental region (SCR) in China defined by JOHNSTON and KANTER (1990), KANTER (1994), and JOHNSTON (1996a). The east part of the Sino–Korean platform (the Korean Peninsula and adjacent gulfs and seas) is also regarded as SCR (KANTER, 1994). Two other areas in eastern Asia, including Mongolia, in northeastern Asia and the Indo–China block in southeastern Asia, can also be regarded as SCRs but are not discussed in this paper.

The present paper first outlines the fundamental concepts and definitions for SCR earthquake studies, followed by a general description of eastern Asia

tectonics and the position of the SCB relative to the overall eastern Asian tectonics. The neo-tectonic features, deformation pattern, and geophysical findings in the SCB are then more thoroughly discussed. Next, the seismicity in the SCB is presented and related to other geophysical and tectonic features and to possible SCR seismogenic models. Finally, the seismic hazards in the SCB are discussed in terms of probability of strong ground motion and potential economic loss. A major contribution of this paper is the compilation of an inventory of historic moderate to great earthquakes in the SCB. Most of the listed entries are not widely available in English literature.

This paper attempts to answer the following questions:

(1) Why the Yangtze platform is a SCR but not the Sino–Korea platform?
(2) Why the southeastern China coast is more seismically active than most areas of the Yangtze platform?
(3) Which SCR seismogenic model works for the SCB?
(4) What is the most accurate way to estimate seismic loss in the SCB?

2. A Global Inventory of SCR Earthquakes

The term Stable Continental Region (SCR) is considerably more restrictive than the term intraplate, due to the exclusion of the oceanic intraplate crust and intraplate continental regions where active tectonics are currently going on (JOHNSTON and KANTER, 1990). SCR includes the continental nuclei, the Archean cratons of North America and South America, Africa, Europe, Asia, India, Australia, and their associated Proterozoic terrenes, Paleozoic fold belts, and Mesozoic/Cenozoic passive margins. Regions that were recently geologically active are also excluded. Several factors are used to define SCR worldwide.

(1) Old in age – Precambrian cratons and Paleozoic folding belts, which together comprise about 72% of SCR crust. The remaining 28% are crust that has undergone Phanerozoic (< 570 Ma) extension. Passive continental margins are the dominant component of SCR extended crust. Failed intra-cratonic rift zones are the minor component in terms of area however the major contributor in terms of seismic moment release (JOHNSTON and KANTER, 1990);
(2) low seismic moment release;
(3) low heat flow;
(4) greater values of averaged crustal thickness;
(5) lower inelastic attenuation;
(6) lower deformation rates; and
(7) effective transmission of tectonic stress arising from plate boundaries, characterized by a relatively uniform horizontal compressive stress regime with orientation in rough agreement with inferred absolute plate velocity vectors.

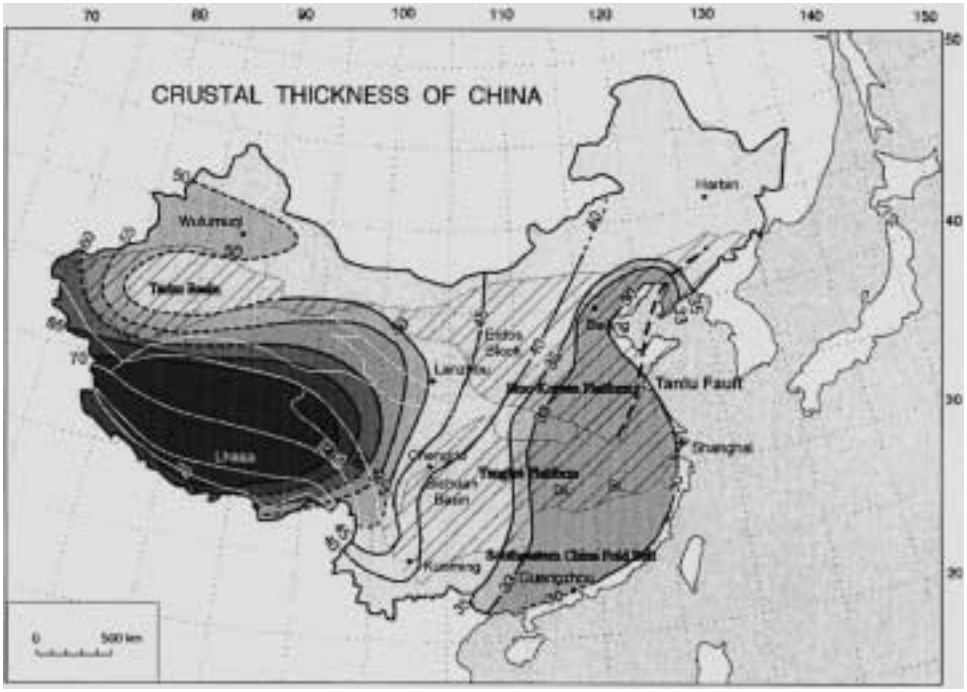

Figure 1
Contours of crust thickness of continental China, with superposition of the locations of fold belts, and Precambrian platforms (hatched area). The Yangtze platform and the southeastern China fold belt form the South China block (SCB) discussed in this paper (modified from LI and MOONEY, 1997). The Tanlu fault (broken line), the locations of the Erdos block, Sichuan Basin, the Dongting Lake (DL), and the Boyang Lake (BL) are also shown.

JOHNSTON (1996a) defined nine continental-scale SCRs in Africa, Antarctica, Asia, Australia, China, Europe, and North and South America. The SCR in China is shown in Figure 1. In Asia the SCRs include China, India, Mongolia and Indo–China. The SCB discussed in detail in the following sections is actually the southern part of the SCR of China defined by JOHNSTON and KANTER (1990) and KANTER (1994). The justifications for choosing only the SCB, not the Sino–Korean platform for discussion, are as follows. First, tectonically, the Korean peninsula should be viewed as part of the Sino–Korean platform formed in Precambrian time that belongs to the North China block. Even though the Korean peninsula is seismically quiet and tectonically stable in modern time, the western part of this platform has experienced active tectonic evolution in Mesozoic to Cenozoic time (MA, 1989). JOHNSTON and KANTER (1990) and KANTER (1994) excluded most parts of this platform from SCR. Second, information on tectonics and detailed seismicity for the Korean peninsula is relatively sparse. For these two reasons, the present paper focuses on the South China block (SCB). The spatial boundary of the SCB is given in the next section.

3. South China Block – Its Relevance in a Large Tectonic Picture

First, it is necessary to clarify the most frequently used geological terms in this paper. The platform is a stable geological unit crystallized in Precambrian time but then subsequently overlain by sediments. The shield area is a platform without sedimentary cover resulting from continued uplift through geological time. Young platform means that crystallization occurred in Paleozoic time. In this section we define the spatial extend of the South China block (SCB) discussed in this paper.

3.1. Spatial Definition of the South China Block

The western boundary of the SCB can be taken as the line passing through the three largest cities in central China, which are, from north to south, Lanzhou, Chengdu, and Kunming (see Fig. 1, approximately the longitude of 104°E). However, because the western boundary is quite gradational, to be conservative, only tectonics and earthquakes east of 105°E are discussed in this paper.

The northern boundary of the SCB can be defined as the Qinling–Dabie suture zone between South and North China. This ancient suture zone, separating the Sino–Korean platform to the north from the Yangtze platform to the south, is a significant intra-continental orogenic zone caused by cratonic interaction (LI, 1994). The paleomagnetic poles, which range in age from late Carboniferous to Tertiary and even modern time, have been compiled by SEGUIN and ZHAI (1995) to establish the refined apparent polar wander path of the Sino–Korean platform. The Sino–Korean platform and the Yangtze platform started to collide in late Permian time near the eastern part of the Qinling–Dabie fold belt (SEGUIN and ZHAI, 1995). During late Triassic to early Jurassic time, the Sino–Korean platform rotated counter-clockwise about 80 degrees, resulting in a gradual collision between the Sino–Korean and Yangtze platforms that progressed westward with the two blocks finally connecting together in Jurassic time (SEGUIN and ZHAI, 1995).

The SCB also includes the areas east of the border formed by the Tancheng–Lujiang (Tanlu) fault zone and the northwest boundary of the North Jiangsu–South Yellow Sea Basin (see Fig. 1, also Figure 1 of CHUNG *et al.*, 1995; KANTER, 1994). The Tanlu fault zone is one of the major tectonic structures in eastern China formed in the late Archean era. Its south end is near the eastern flank of Dabie Mountain near Tongcheng in the Anhui Province. The north–northeast striking Tanlu fault zone extends from Tongcheng in the south, through Jiangsu and Shandong provinces, crosses the Bohai Gulf into the Liaodong Peninsula, and ends near Huadian in Liaoning Province in the north. The total length of the fault is about 2000 km. Nevertheless, when defining the boundary of the SCB, the triangular shaped area bounded by the Tanlu fault zone to the west and the northwest boundary of the North Jiangsu–South Yellow Sea Basin to the east is excluded for its high deformation rate and high seismicity in modern time (KANTER, 1994).

The SCB studied in this paper includes the continental shelf in the Yellow Sea and most parts of the East China Sea until the continental slope to the east. The Neocathaysian massif, a piece of detached Precambrian basement resulting from mid- to late-Mesozoic rifting (JUAN, 1986), separates the Yellow Sea and the East China Sea. The definition of the eastern boundary is vague, because there is neither much modern seismicity nor historical data for the remote East China Sea. Taiwan, sitting on a plate boundary, is at a critical location (the northwest corner) in the interaction between the Philippine Sea plate and the Eurasian plate. It is experiencing high deformation rates and intensive seismicity. The seismicity near Taiwan along the plate boundaries has been plotted in Figure 4 for reference.

The southern boundary of the SCB is the continental slope south of Hainan Island, extending northwesterly into Vietnam and the Guangxi Province of China along a high deformation rate zone separating the SCB and the Indo–China SCR. Therefore, the SCB includes part of the South China Sea and the Gulf of Tonkin.

3.2. Comparison with the North China Block

The Sino–Korean platform, which is the major component of the North China block, was consolidated in the Archean time (~3 Ga, see MA, 1989), or at least as early as the Yangtze platform, which is the kernel of the SCB. However, the Sino–Korean platform has undergone deformation and seismic activity in subsequent geologic times. Since the Tertiary, large areal subsidence has occurred east of the Taihang–Funiu Mountains, whereas to the west of it there were periodic uplifts (the Shanxi graben system). In addition, graben systems formed in Quaternary time around most of the periphery of the Erdos block (see Fig. 1). Some neotectonic activities have continued to modern time (e.g., the Shanxi graben since Neogene age). All these tectonic activities clearly indicate that the North China block cannot be classified as a stable continental region (SCR).

3.3. Geological History of Continental China

The continental evolution of China consists of 8 orogenic cycles and 18 rifting and openings (YANG *et al.*, 1984; DING, 1991). In general, the region was dominated by orogeny prior to the late Permian/early Triassic, and by extension in subsequent time (Fig. 2, also see YANG, *et al.*, 1984). In the smaller eastern China region, however, the North China platform was dominated by extension and opening since the Luuliang Orogeny which occurred ~2.0 Ga in early Proterozoic time. Meanwhile, South China was dominated by continuous compression and had undergone weak to moderate uplift with crust accretion toward the southeast from the Yangtze platform (DING, 1991). The southeast China fold belt is located in the backarc region of the Philippine–Eurasia collision zone. It was attached to the Yangtze platform during Cambrian time as a series of fold zones.

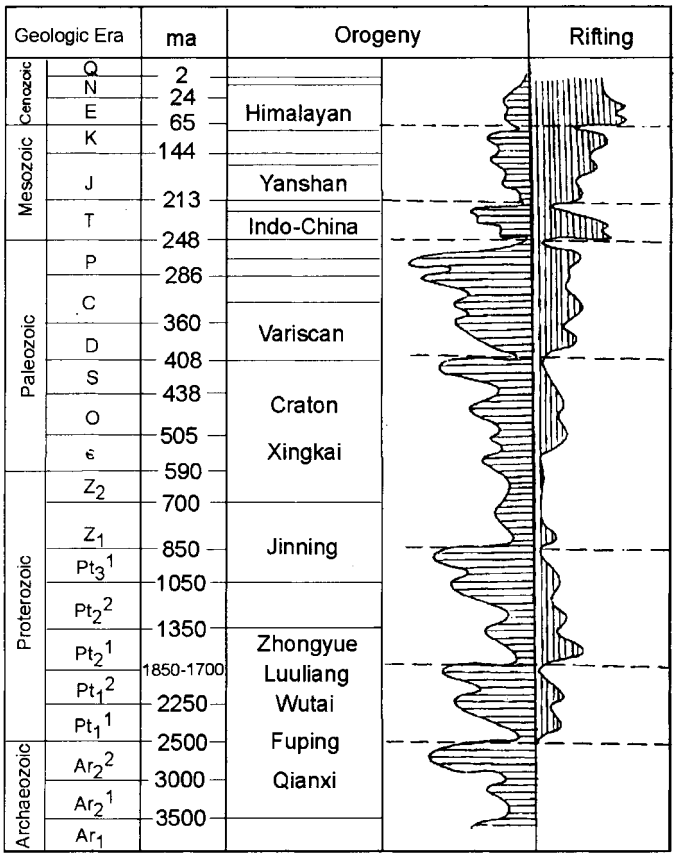

Figure 2
The column diagram of tectonic evolution history showing the orogeny and rifting of China continent (after YANG *et al.*, 1984).

The overall picture of neotectonic evolution in China since 40 Ma ago (Eocene Epoch) can be depicted as follows. The rapid uplift of the Tibetan plateau (especially since Pleistocene) was accompanied by numerous strike-slip faults rupturing the surrounding areas under strong compression. The northwest China region was characterized by secondary high ranges and depressional basins. The northeast China region was characterized by rifting and opening. South China was characterized by moderate uplifting. The East China Sea and Okinawa Islands together formed an active rift zone. The South China Sea was an oceanic basin with relatively thick sediments since some 10 Ma ago in the Himalayan Orogeny in the Neogene period. Except for a couple of areas, such as the Dongting Lake and Boyang Lake (Fig. 1), most regions in the SCB have undergone a vast uplifting since the Tertiary, and the entire region has been uplifted since Quaternary time.

The collision between the Indian and the Eurasian plates is the controlling factor in the neotectonics of eastern Asia. The stress field generated from this collision is in a sectoral pattern radiated from the suture zone of the India-Himalayan mountain range. To the north, the northward movement of the Tibetan plateau generates a large compression in the Tarim basin block which has resulted in a secondary orogeny of the Tianshan mountain range. To the east, the northward motion produces a gigantic, right-lateral shear zone, known as the north–south seismic zone, which divides China tectonically into western and eastern China. This north–south seismic zone is generally accepted to have resulted from the resistance to the motion of the Tibetan plateau by a mantle uplift beneath Sichuan basin (a barrier to resist easterly motion with thinner crust, see Fig. 1) and the Erdos block (which is stable and cold, see Fig. 1). The resistance of the Sichuan Mantle Uplift is so high that the eastward mass flow from the lower crust of the Tibetan plateau has to change direction to move southeasterly (ROYDEN *et al.*, 1997). The north–south seismic zone has absorbed the strong push from the west, so that the deviatoric stress in the SCB is low and consequently the SCB is characterized by a low deformation rate and low seismicity.

4. Tectonics in the SCB – A Detailed Picture

4.1. Tectonics within the SCB

The Yangtze platform is one of the three oldest stable platforms in the China continent (the other two are the Sino–Korea platform and the Tarim Basin) (ZENG *et al.*, 1995). The Sino–Korean platform solidified in the early middle Proterozoic (1700 Ma), whereas the Yangtze and Tarim platforms solidified in the late Proterozoic (700 Ma). Recently acquired geophysical data indicate that the Yangtze platform collided with the Sino–Korean platform to create the Qinling range along the suture zone in the middle Jurassic (LI, 1994).

The complete tectonic record of crustal growth from Archean to Cenozoic is preserved in the South China continent. Within the Yangtze platform, which forms the kernel of the whole SCB, the Precambrian basement is composed of gray gneiss, early Proterozoic komatiitic greenstone, and late Proterozoic ophiolite and greenstone. At the present time they are relatively cold and stable with high seismic velocity and electric resistivity (XIE *et al.*, 1997). Along the southeast China coast, the igneous rocks (alkaline granitic and syenitic belts, and various types of basalt) resulting from the Mesozoic to Cenozoic activities, are characterized by relatively high heat flow, lower seismic velocity, and higher electric conductivity (XIE *et al.*, 1997; WANG *et al.*, 1995). A super breakup zone along the southeast China coast, which may have cut through the entire upper mantle, is regarded as the major focus of heat transport (XIE *et al.*, 1997).

4.2. Major Geophysical Features in the SCB

The 'Lithospheric Dynamics Atlas of China' (MA, 1989) summarizes the major scientific findings based on tectonic studies of the last several decades regarding China's continental dynamic features. The crustal thickness, seismic velocities, heat flow, and tectonic stress in the SCB are briefly discussed below.

Mainland China can be divided into eight blocks, based on the crustal thickness expressed by Moho depth variations. The Moho depth within any one block is relatively uniform; however, it changes abruptly from one block to another (ZENG *et al.*, 1995). The southeastern China fold belt consists of exotic terrains that attached to the Yangtze platform during the Craton (460 Ma in Ordovician) and the Variscan (320 Ma in Carboniferous) orogenies. The SCB can be divided into 4 regions with different crustal thickness. From west to east, they are: (1) the Upper Yangtze platform, 40–46 km; (2) the Xuefeng Mountain transition belt in N–S direction, 34–38 km; (3) the Lower Yangtze platform, 32–34 km; and (4) the Southeast China coast, 30–32 km (ZENG *et al.*, 1995). The Lower Yangtze platform, combined with part of the southeastern China fold belt, dominates the SCB with an averaged crustal thickness of 33 km (Fig. 1, also see LI and MOONEY, 1997). In the East China Sea and South China Sea (including the Hainan Island) the crustal thickness is 26–28 km. More recent crustal thickness studies (LI and MOONEY, 1997) in general confirm previous results (ZENG *et al.*, 1995). The new studies also reveal an intermediate mafic lower crust with *P*-wave velocities of 6.9–7.0 km/sec. This layer is thicker in the South China region than in the North China region (Fig. 3, also see LI and MOONEY, 1997).

In general, the quality of the heat flow data is poor and the spatial distribution of heat flow observations is sparse and uneven in the entire China continent. Until 1983 the number of published heat flow values was only 181 (DING, 1991). The amount of data can be increased if the observed temperature gradients in a borehole are used with thermal conductivity values measured for similar rock samples cored from nearby boreholes. By including this type of data, WANG *et al.* (1995) determined the heat flow values for 41 boreholes in the Lower Yangtze area. The South China block and the Lower Yangtze area have a background heat flow value of about 60 mW/m^2 (POLLACK *et al.*, 1993; WANG *et al.*, 1995). In the north Jiangsu Basin and along the Tanlu fault zone, a higher averaged heat flow value of close to 70 mW/m^2 has been observed, which is an indication of tectonic and magmatic activities in Mesozoic time (WANG *et al.*, 1995).

The tectonic stress field in the SCB, as indicated in the World Stress Map (ZOBACK, 1992; MUELLER *et al.*, 1997) inferred from active faulting, borehole breakouts, and seismic focal mechanisms, shows that the SCB is generally in a strike-slip to normal faulting regime. The horizontal principal compressive stress in the SCB is directed NW to WNW. This stress orientation agrees well with the radial pattern of crustal movement resulting from the Indian–Eurasian collision along the

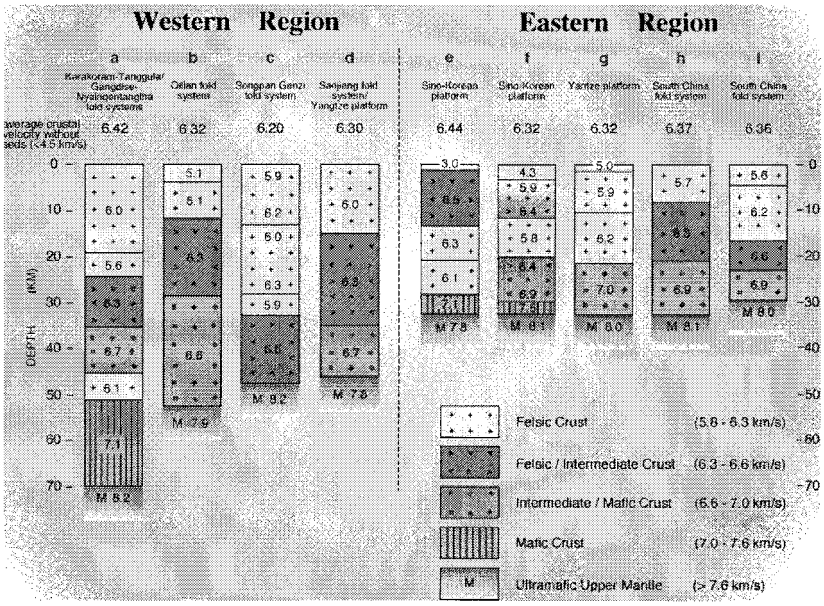

Figure 3
The column diagram of crust composition of China continent (from LI and MOONEY, 1997).

Himalayan orogenic belt, with the possible addition of compression generated from the westward subduction of the Philippine Sea plate, which occurs southeast of the SCB.

5. Seismicity Pattern and Features in the SCB

The historic data (see Appendix A) are based on the 'Atlas of the Historical Earthquakes in China' (hereinafter AHEC) compiled by the Institute of Geophysics, State Seismological Bureau and the Institute of Chinese Historical Geography, Fudan University (1983). Appendix A also includes events recorded in the provisional earthquake catalog for regions close to Hong Kong compiled by MUSSON (1991, 1995, hereinafter MUSS) of the British Geological Survey. During the compilation of Appendix A, if a particular historic event was included in both AHEC and MUSS, the information provided by AHEC is adapted. All MUSS events marked by 'weak data' (poor constraints on iso-intensity contours) and 'dam event' (associated with the impoundment of a reservoir) are not included in Appendix A. Epicenters of all historic events in Appendix A are depicted by open circles in Figure 4. The modern instrumentally recorded events (filled circles in Fig. 4) are those that have occurred from 1990 to 2000 with minimum magnitude of 3.0 extracted from the Council of the National Seismic System (CNSS) catalog managed

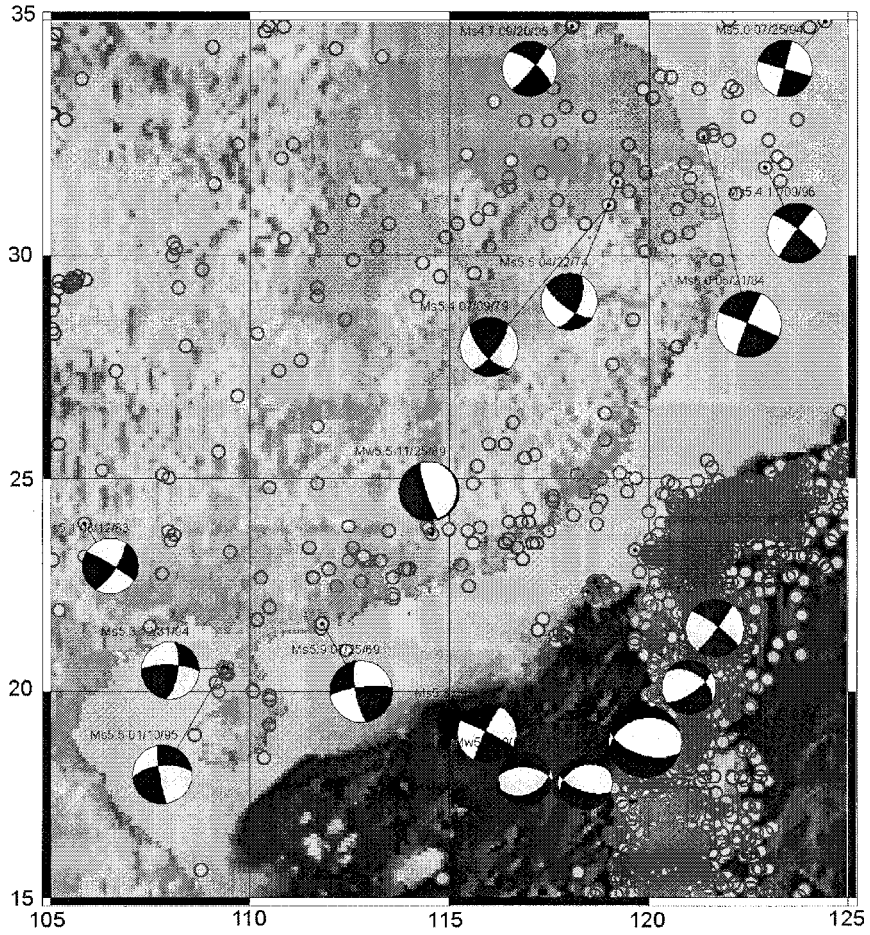

Figure 4
Map of seismicity in the South China block. Open circles denote events from the historic data from 1000 AD to the 1920s listed in Appendix A. Modern seismicity (filled circles) are from the National Council of Seismic System catalog (1990–2000). The focal mechanism solutions are from Harvard CMT Catalog, with additions of the 1969 Yangjiang earthquake from BRANTLEY and CHUNG (1991), and the 1974 Liyang earthquake from CHUNG *et al.* (1995).

by the University of California at Berkeley. Earthquake focal mechanisms plotted in Figure 4 are extracted from the Harvard University Centroid Moment Tensor (CMT) Catalog.

5.1. Historical Seismicity Data

During the approximately 4000 years of written history in China, earthquakes have always been an important natural phenomenon recorded in official documents and literatures. In the SCB, many earthquake records can be found in different levels

of historical documents. The Atlas of the Historical Earthquakes in China (AHEC, 1983) compiled the historical data and assigned the maximum intensity, and the iso-intensity distribution when data are good enough, to each historical event. Though AHEC's compilation of historic earthquakes has spanned a period of more than three millennia, not surprisingly, the catalog is more incomplete for earlier years. Appendix A lists a total of 129 historical earthquake events in the SCB from 1000 AD to the 1920s extracted from AHEC and MUSS. The reason is that the historic records are more uniform and complete for the last 1000 years, starting from the Yuan Dynasty in Chinese history. For most of the events in AHEC, an iso-intensity map accompanies the record. The magnitudes of the historic events were determined from the value of the maximum intensity:

$$\boldsymbol{M} = 0.58 I_{\max} + 1.5.$$

To verify these magnitudes with respect to values obtained by other more advanced quantitative measures of intensity for historic earthquakes, we computed the moment magnitude M for each event based on an approach proposed by JOHNSTON (1996b). With a regression between the maximum intensity and the seismic moment for SCR earthquakes instrumentally recorded in recent years, JOHNSTON (1996b) obtained the following relation to derive the seismic moment M_0 from the maximum intensity, $I_{\max}$, of a historic event:

$$\log(M_0) = 19.36 + 0.481 I_{\max} + 0.0244 I_{\max}^2$$

then, by the relation between the moment and the magnitude (HANKS and KANAMORI, 1979)

$$\boldsymbol{M} = \frac{2}{3}\log(M_0) - 10.7$$

the moment magnitude can be obtained. JOHNSTON (1996c) has successfully applied this approach to study the magnitudes of the three historic earthquakes that occurred in the 1811–1812 winter in the New Madrid seismic zone in central North America. Appendix A included the moment magnitude acquired by this approach for events whose maximum intensity is available. In general, the magnitudes gained by this approach are systematically smaller than those originally given by AHEC and MUSS.

5.2. Instrumentally Recorded Seismicity

The instrumentally recorded earthquake events in the SCB shown in Figure 4 were extracted from the National Council of Seismic System (NCSS) catalog maintained by the University of California at Berkeley. The events are those which occurred in this area between 1990 and 2000 with magnitudes greater than 3. As a reference, events that occurred along plate boundaries between the Eurasian and the Philippine Sea plates are also shown in Figure 4. In general, events southeast of the

intersection of longitude 120°E, latitude 20°N belong to plate boundary events. From Figure 4 it is clear that the SCB seismicity is considerably sparser than that along plate boundaries. Nevertheless, a number of seismicity belts with a relatively high concentration of earthquake events can be identified. (1) The Southeast China Coast seismic zone in Guangdong and Fujian provinces: This zone coincides with the southeast China coastal fold belt. Seismicity in this seismic zone is probably associated with the Eurasia–Philippine collision. Tectonically, the coastal seismic zone coincides with the coastal fold belt and belongs to a passive margin in terms of plate tectonics settings. (2) The Southern Yellow Sea seismic zone: This zone seems to be associated with continental shelf basins. This zone has been relatively seismically active compared to most other regions of the SCB. From 1764 to 1984, 19 earthquakes have occurred with surface wave magnitude greater than 6, and 29 events with surface wave magnitude between 5 and 6 occurred in this region (CHUNG and BRANTLEY, 1989). (3) The seismic zone in Downstream Yangtze River Plain: Seismicity in this zone is possibly associated with Tertiary rifts and basins.

The SCB events are basically all crustal events with focal depths less than 33 kilometers. Unfortunately, the depth constraint on these events is poor due to sparse seismic station coverage and poorly known crustal velocity structure. No detailed discussion on depth distribution of the SCB earthquakes is attempted in the present paper.

5.3. Focal Mechanisms of the SCB Earthquakes

Due to the relatively low level of seismicity and the sparseness of local and regional seismic station network, only a handful of the SCB events can be used to exercise focal mechanism determination. In Figure 4, eleven focal mechanisms were plotted for the continental SCB. Two of the 11 solutions, the 1969 Yangjiang earthquake in Guangdong Province, and the 1974 Liyang earthquake in Jiangsu Province, were published by BRANTLEY and CHUNG (1991), and CHUNG *et al.* (1995), respectively. These two events occurred before 1976, the starting date of the Harvard CMT catalog coverage. The remaining 9 solutions are however, from the Harvard CMT catalog. Besides these eleven, 6 more solutions for events which occurred near the continental slope in the South China Sea were also plotted for reference, however, it is arguable whether they belong to the stable continental region earthquakes. Most of the 11 SCB events display a strike-slip fault rupture style. The event that occurred on November 25, 1989 in Heyuan, Guangdong Province (longitude 114.57°E, latitude 23.72°N) is a dam event associated with reservoir impoundment. It is essentially a normal faulting event striking NNW with a very steep dip angle. The two earthquakes that occurred in Liyang, Jiangsu provinces in 1974 and 1979 show a small component of reverse faulting superimposed with the dominant strike-slipping. Nevertheless, from this figure it is clear that all focal mechanisms for the SCB events that occurred in the last 30 years exhibit a group of

faulting styles consistent with the northwesterly oriented principal compressive stress in a normal to strike-slip faulting regime. The tectonic stress field in the SCB, as many have indicated, is a result of the stresses caused by Indian–Eurasian collision west of the SCB, and the subduction of the Philippine Sea plate, east of the SCB.

The focal mechanisms for events that occurred near the continental slope in the South China Sea show mostly normal faulting style, consistent with the gravity-driven NS extension expected near a steep slope. The inferred horizontal compressive stress is closer to east–west direction, which possibly results from the westward subduction of the Philippine Sea plate to the east of the continental slope.

5.4. Some Significant Features of the SCB Earthquakes

Based on the above description and summary of the SCB earthquake events recorded by both historical records and modern instruments, several striking features can be characterized for the SCB seismicity. First, most of the clustered seismicity definitely coincides with geological and geophysical features. For example, both the southeast coastal fold belt and the north Jiangsu basin have a higher heat flow value and both also have a higher seismicity. In general, a relatively high value of heat flow indicates relative recency of the last tectonic or magmatic activities in geological history. LIU and ZOBACK (1997) argued that possibly, a slightly higher geotherm may be a critical factor in fostering the great historical earthquakes in the New Madrid seismic zone in eastern North America, another stable continental region. Second, most SCB earthquakes might occur on faults or other planes of weakness formed in pre-existing tectonic structures. The Liyang earthquakes, for example, occurred at the intersection of two faults normal to each other inside a pre-existing later Mesozoic to late Tertiary extensional graben (CHUNG *et al.*, 1995). This fact supports TALWANI's hypothesis (1999) that the fault intersections are potential hotbeds for SCR earthquakes. Another striking tendency is that SCR earthquakes usually occur along structures that have optimal orientation with respect to the maximum horizontal stress axes; it does not matter whether the structures are major or secondary. Again, taking the Liyang earthquakes as an example, it is inconclusive which is the rupture plane between the two nodal planes for the 1979 event, although, at least, it is quite certain that the 1974 event ruptured the secondary NW oriented fault (CHUNG *et al.*, 1995). The possible reason is that it is easier for a shear failure developing on the NW plane under the regional E–W principal compressive stress.

6. The SCB Seismic Hazard

The SCB is one of the most populous regions in the entire Eurasian continent (Fig. 5a). Although the seismic hazard is relatively low in this region (Fig. 5b),

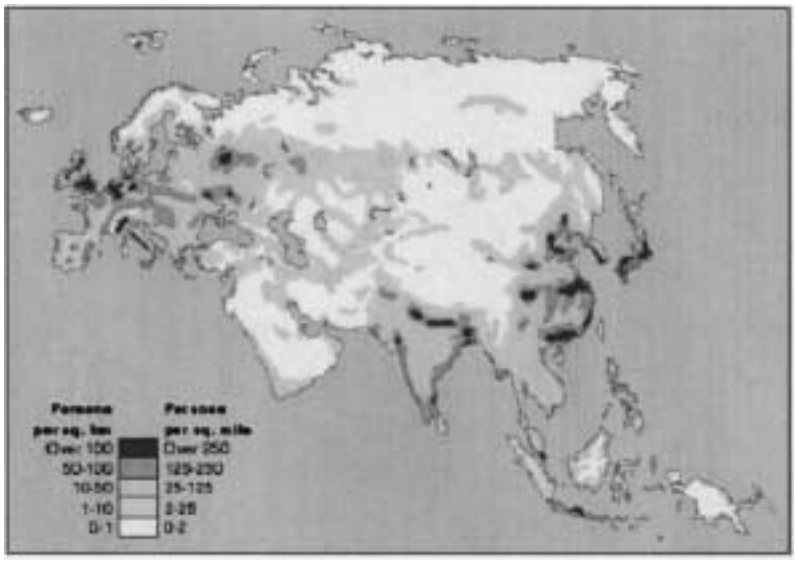

Figure 5a
The population distribution in continental Eurasia (extracted from the web site at URL: http://www.larouchepub.com/lar_glazyev_2513/1EurasiaPopulationColor.gif).

seismic hazard mitigation is of particular significance by considering the rapid social and economic development in this region. The discussion of the seismic hazard in the SCB initiates from a discussion of the seismic hazard at the national level.

6.1. Historic Development of National Seismic Hazard Assessment in China

The first national seismic hazard assessment project in China was conducted originally in conjunction with the former USSR, beginning in the early 1950s. The assessment was guided by two important principles: (1) Earthquakes of similar magnitude will recur where they originally occurred; and (2) regions of similar tectonic structure are subject to similar seismic potential. In 1977, China completed the second generation of the national seismic hazard map based on the seismic and seismotectonic data available at that time. This project also forecasted the maximum seismic intensity for a period of 100 years. The hazard map was used to develop a new national building code for China. In 1992, China published the third generation of its national seismic hazard map. Starting with the map published in 1992, China began to use CORNELL's (1968) probabilistic approach to seismic hazard analysis instead of the deterministic approach utilized in the previous two versions. The 1992 map depicts intensities with an exceedance probability of 10% for a period of 50 years on a given site with averaged conditions.

As one important component of the Global Seismic Hazard Assessment Project (HSHAP), a new national seismic hazard map of China has just been completed

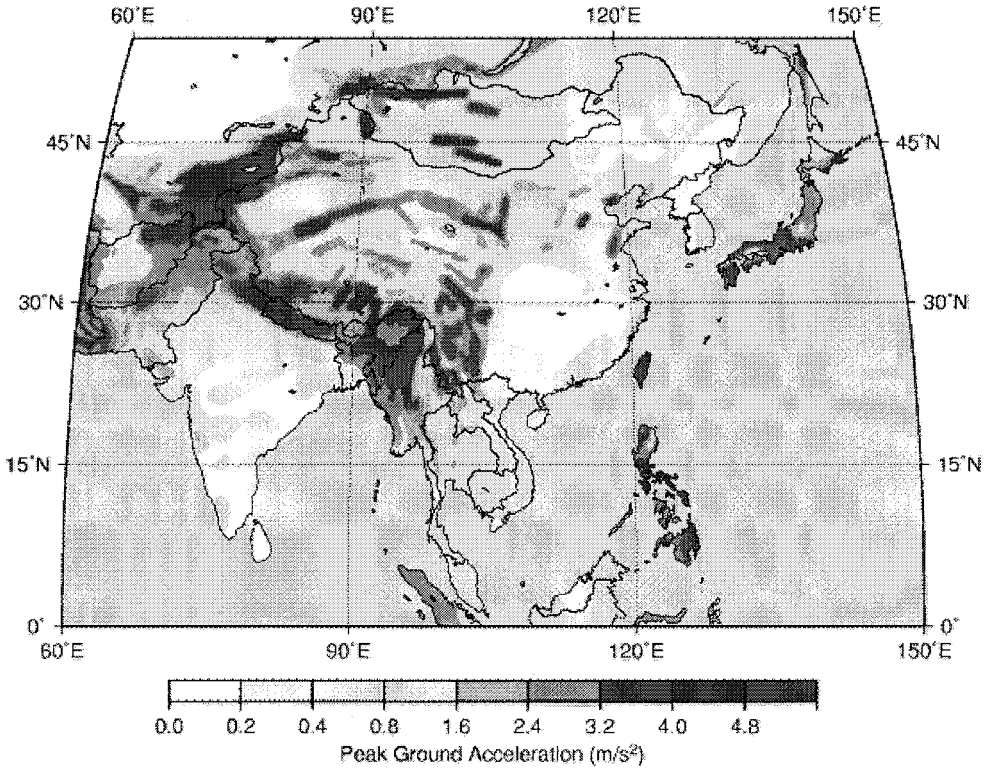

Figure 5b
The seismic hazard map of Asia depicting peak ground acceleration (PGA), given in units of m/s^2, with a 10% chance of exceedance in 50 years. The site classification is bedrock (extracted from the Global Seismic Hazard Assessment Program web site at URL: http://seismo.ethz.ch/GSHAP/eastasia/asiafin.gif).

(Fig. 5b) by the State Seismological Bureau (now the China Seismological Bureau) in 1999 (ZHANG *et al.*, 1999). In the new map the seismic hazard was depicted with the peak ground acceleration (PGA), instead of intensity grades. The seismic hazard map of the SCB shown in Figure 6a was extracted from the Global Seismic Hazard Map published by GSHAP (GIARDINI *et al.*, 1999; ZHANG *et al.*, 1999). The map shows clearly that for most parts of the SCB, especially in the kernel part, the seismic hazard in the Yangtze platform (see Fig. 1) is extremely low. The expected peak ground acceleration (PGA) on a typical bedrock site is only 0–0.2 m/s^2 at a 10% probability of exceedance in a 50-year period. Higher PGAs (0.2 to 0.8 m/s^2) are assigned to coastal areas in Guangdong, Fujian, and Zhejiang provinces.

6.2. An Alternative Way to Estimate Earthquake Economic Loss

Probability forecasting of earthquake losses should ideally include estimates of two types of losses – economic and social losses. The economic loss encompasses all

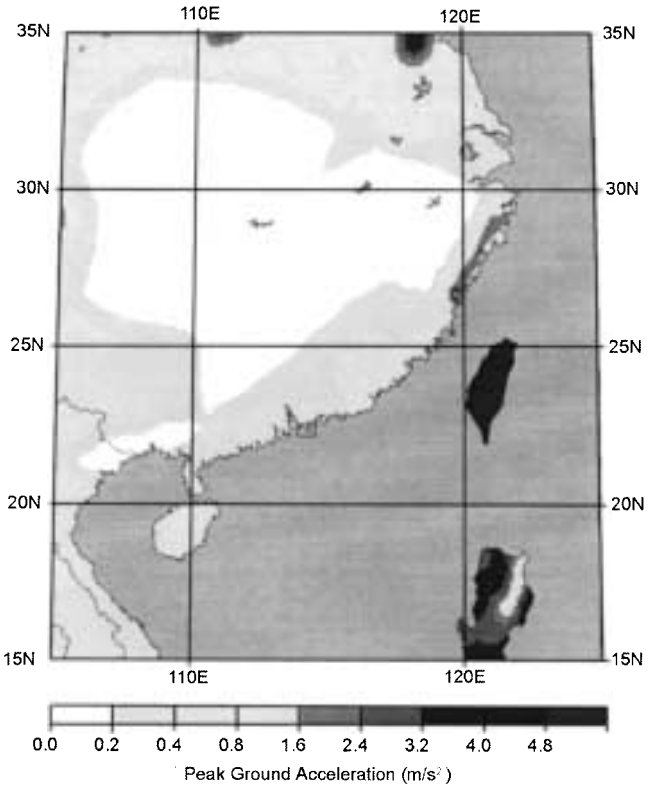

Figure 6a
Seismic hazard in the South China area in terms of peak ground acceleration (PGA) on bedrock site. This map was extracted from the database managed by the Global Seismic Hazard Assessment Program (modified from ZHANG *et al.*, 1999).

physical damages of buildings, lifeline structures, and properties, as well as deprivation of revenues from business interruption, which accounts for a large portion of the total economic loss. In contrast, social losses include casualties and injuries to the residents in the affected region, as well as the long-term negative effects on people's physical and mental health. The social losses are highly variable from case to case and it is difficult to derive an objective estimate. For this reason, only the economic losses are considered in the discussion of earthquake losses.

Most approaches for estimating earthquake economic losses require a detailed inventory of the facilities and structures within the study region. Nevertheless, the detailed inventory information is hard to access in many regions and nations, and therefore forecasts of economic losses will have high uncertainties. It is imperative to explore alternative approaches for earthquake loss forecasting that rely less on detailed inventories of local structures and geological information and more on data that is readily available. Based on these arguments, CHAN *et al.* (1998) conducted an

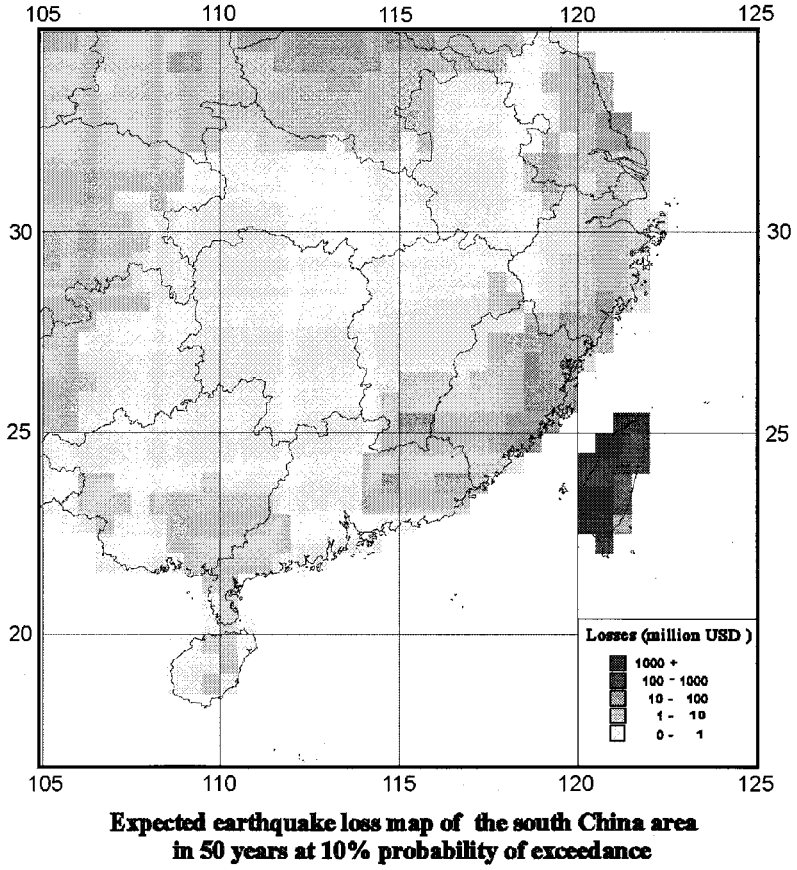

Figure 6b
The seismic economic loss in the South China area (from CHAN *et al.*, 1998). The losses in millions of US dollars are the total loss in a $0.5° \times 0.5°$ cell.

assessment of global seismic loss based on macroeconomic indicators such as the gross domestic product (GDP) or the gross national product (GNP). They argue that because the GNP includes overseas income earned by the residents in an area and, because such overseas earnings are unlikely to be affected in a local earthquake event, the GDP is the more appropriate index to use for seismic hazard analysis. For a given area, the estimated loss is formulated as

$$L = \sum_I P(I) \cdot F(I, \mathrm{GDP}) \cdot \mathrm{GDP}$$

where L is the economic loss; $P(I)$ the probability of occurrence of earthquakes with intensity I; and $F(I, \mathrm{GDP})$ the area's vulnerability to earthquake damage.

Because the GDP is close to linearly related to the population density, CHAN *et al.* (1998) proposed using the population density times the conversion factor as the

inferred GDP in areas where GDP data are not available. Based upon an earthquake catalog database containing 29 entries with both economic loss and GDP since 1980 for MMI > VI, they advanced their analysis to seek the correlation between potential economic loss resulting from earthquake hazard and GDP to establish the probability estimation of economic loss.

Figure 6b is the economic loss map for the SCB, a portion of the global economic loss map generated by this approach. Comparison with the newly compiled GSHAP global seismic hazard map (GIARDINI *et al.*, 1999) in the SCB area reveals differences for estimation of the hazard. To the first order, both maps depict the Yangtze platform with the lowest hazard. However, they indicate significant differences in characterizing the seismic hazard in coastal areas. The GSHAP map shows the highest PGA along the Zhejiang coast (Fig. 6a), whereas the economic loss map based on GDP depicts the highest losses along the Fujian coast crossing the Taiwan Straits (Fig. 6b). The reason for the difference could be that the economic loss map based on the GDP is weighted more by the high population and economic blooming in Fujian Province, whereas the GSHAP hazard map emphasizes more the possible maximum groundshaking.

6.3. The Significance of the SCR Earthquakes in Terms of Seismic Hazard

SEEBER and ARMBRUSTER (1998) generalized the seismogenic characteristics of the SCR earthquakes. Some of these features are discussed here in conjunction with the SCB seismicity characteristics presented in the last section.

Potential seismogenic faults are plentiful and widely scattered in the SCR. In the SCB, seismicity spreads over all parts of the region, although with a sparse distribution. The magnitude of a potential damaging earthquake may be low; however, because of the vast spatial distribution, low-degree seismic hazard can be posed anywhere in the SCB. This is in sharp contrast to the situation along plate boundaries where earthquake focal locations are concentrated in a narrow zone so that forecasts can be more precise in terms of location, though the forecasting of time is not realistic by the current understanding of seismogenic process.

The SCRs have lower seismic attenuation (e.g., NUTTLI, 1973) so a larger area can be affected. The SCR earthquakes are mostly shallow; therefore, they can cause more damage than inter-plate earthquakes of similar size because not only is the attenuation lower, but also seismic energy can be released closer to the surface in the SCR than at plate boundaries. All of the 11 SCB events have a focal depth of less than 33 km. Detailed focal mechanism studies show that the focal depth of the 1969 Yangjiang earthquake is only 9 km (BRANTLEY and CHUNG, 1991), and 12 km and 8 km, respectively, for the 1974 and 1979 Liyang earthquakes (CHUNG *et al.*, 1995).

Many scattered active faults with low slip rates seem to violate the principle of strain softening, and suggest a mechanism that stresses are building up locally. Continent-wide patterns of stress orientations suggest that instead of forces applied

at the boundaries of the stable continental lithosphere, SCR tectonics may be driven by a combination of both boundary forces (mostly in a horizontal direction) and local forces (in both vertical and horizontal directions). All of the above considerations have added more complexities and uncertainties to seismic hazard assessment in the stable continental regions.

7. Discussions Regarding the SCB Seismogenic Models

In general, the seismic activity in the SCB is much less than at its plate boundaries, as example, the arc-continent collision zone between the Eurasian continent and the Philippine Sea plate to the southeast of the SCB. The lack of intensive seismicity can be attributed to the low to intermediate stress level as indicated by the strike-slip to normal faulting styles in the SCB. No significant thrust faulting has been found in the entire region. Moreover, the major tectonic features are mostly oriented in the NE direction, and essentially normal to the direction of the horizontal principal compressive stress. This relative orientation demands higher stress level to rupture the NE oriented faults and structures so that failures on these planes are more difficult. Rock mechanics has clearly indicated that for a given rock type the value of the compressive strength is greater than that of the shear strength, and both of them exceed the tensile strength (e.g., JEAGER and COOK, 1979). Thus it is not surprising to see that under a uniform tectonic stress the SCB earthquakes will rupture the secondary plane whose orientation is favorable to shear or tensile failure rather than rupturing the other unfavorably oriented plane by reverse faulting.

7.1. Seismogenic Models for SCRs

Several seismogenic models have been developed in the last three decades for earthquakes in a stable continental interior. SYKES (1978) proposed a model with a reactivation of pre-existing zone of weakness. Its essence is that the SCR earthquakes tend to rupture old zones with weakness planes under current tectonic stress regime. CAMPBELL (1978) proposed a stress concentration model. He argued that the heterogeneities in the crust could generate secondary stress concentration, such as the stresses surrounding a hard igneous intrusive body. JOHNSTON and KANTER (1990) noticed the coincidence of location of the SCR earthquakes and the failed ancient rift systems on a global scale.

WESNOUSKY and SCHOLZ (1980) indicated that inside the cratonic region the seismicity is essentially diffuse and random. Nevertheless, major seismic zones can be associated mainly with passive margins, fold belts, and ancient rift zones. LIU (1993) and LIU and ZOBACK (1997) proposed the coincidence of high seismicity and relatively high heat flow in intra-cratonic seismic zones such as the New Madrid seismic zone in central North America. TALWANI (1999) proposed a similar model

with the reactivation of zones of weakness, but he emphasized the intersections of two faults normal to each other.

7.2. Seismogenic Models for the SCB

Three significant SCB earthquakes, additional to 12 other worldwide SCR events, were regarded as representative SCR events and discussed by JOHNSTON and KANTER (1990). They argued that these are the largest earthquakes on a moment magnitude scale ever recorded in global stable continental regions, and they all occurred where crust has been stretched and thinned over the past 250 million years (JOHNSTON and KANTER, 1990). Of the three SCB events, the 1604 M7.7 Taiwan Straits earthquake and the 1918 M7.4 Nanao earthquake occurred in passive margins, whereas the 1605 M7.3 Hainan earthquake occurred in a rift zone. Actually, some earthquakes in the southern Yellow Sea seismic zone may have occurred with comparable magnitudes. However, due to remoteness and poor coverage of the historic records for seismic damage on land, no dependable magnitude estimates could be obtained, based upon the available data. Nevertheless, the modern instrument record of events with lower magnitudes indicates that earthquakes in this seismic zone can be associated with active rifting of the Yellow Sea continental shelf basins. Based upon the historic and instrumental records, it seems that among the three seismic zones in the SCB, the southeast China coast seismic zone is associated with passive margin, and the downstream Yangtze River and the southern Yellow Sea seismic zones are associated with ancient or modern rift zones. All earthquakes in these three zones can be explained by the reactivation of the ancient-zone-of-weakness model (SYKES, 1978). Moreover, the downstream Yangtze River seismic zone is also associated with the north Jiangsu Basin whose heat-flow value is higher than the average heat flow in the SCB. The model of lithospheric thinning by anomalously high heat flow (LIU, 1993; LIU and ZOBACK, 1997) can also be used to interpret high seismicity in this region. The models of stress concentration (e.g., CAMPBELL, 1978) appear to have less applicability to the SCB earthquakes.

8. Summary Remarks

In summary, the tectonic background indicates that the SCB is a cool, rigid, and relatively intact crustal block. This statement is supported by a generally low seismicity in the SCB. Nevertheless, significant earthquakes have occurred in this region, some of which have resulted in huge losses in human lives and economics.

Earthquakes in the SCB are associated with three seismic zones. (1) The southeast China coastal seismic zone related to the coastal fold belt in Guangdong–Fujian provinces; (2) the southern Yellow Sea seismic zone associated with continental shelf basins; and (3) the downstream Yangtze River is associated with Tertiary rifts and basins.

The focal mechanisms in the SCB are consistent with strike-slip to normal faulting stress regime with the horizontal principal compressive stress oriented roughly in the NW–SE direction.

A low level of seismicity in most of the SCB region may be caused by the fact that the major tectonic features are oriented normal to the principal compressive stress axis. Under these conditions, major tectonic structures are least likely to be ruptured by compressional failure. Instead of rupturing these poorly oriented major features, the tectonic stress field tends to rupture favorably oriented secondary faults by shear and extensional failures.

The answers to the questions posed at the beginning of this paper can be summarized as follows.

The SCB experiences lower seismic activity for three major reasons; in accordance with their importance, they are: (1) The SCB is generally cold and strong, and no major tectonic activities have occurred there since early Mesozoic time. (2) As the western boundary of the SCB, the North–South seismic zone acts as an insulator to the thrust from the Tibetan plateau, greatly reducing the stress level acting on the SCB. (3) In the SCB, the orientations of the major tectonic features (in the northeast direction) are almost perpendicular to the direction of the modern tectonic stress (in the northwest direction). Because the crust has a substantially higher compressive strength than shear or tensile strengths, the cumulative tectonic stress rather ruptures faults with opening and shear first, before generating reverse faulting failure. Indeed, in contrast with the SCB, in the North China block and the Sino–Korea platform, a number of major neotectonic features have been active since Cenozoic time when the Himalayan Orogeny started 40 to 50 million years ago. The major structures in the North China block are optimally orientated (in the NE direction) with respect to the stress field resulting from the Indian–Eurasian collision in the NE–E direction. This relative orientation between the stress field and the structures favors right lateral strike–slip on the NE striking vertical faults, and extension and opening on the NWN oriented structures (MA *et al.*, 1989; DING, 1991; LIU *et al.*, 1996).

Inside the SCB, the southeastern China coastal fold belt is seismically more active than the Yangtze platform. The possible reason is that the coastal fold belt is a passive margin closer to the collision zone between the Eurasia and the Philippine Sea plates. It is also geologically younger than the nuclei part of the Yangtze platform.

The SCB earthquakes can be elucidated by a number of seismogenic models. Among them, the reactivation of the ancient zone of weakness model (SYKES, 1978), and the model of lithospheric thinning above an area with an anomalously high geotherm (LIU, 1993; LIU and ZOBACK, 1997) seem more appropriate to explain the SCB earthquakes. Apparently, the downstream Yangtze River seismic zone is associated with the north Jiangsu Basin whose heat flow value is higher than the average heat flow in the SCB. In addition, the Liyang earthquakes occurred at the intersection of a pair of pre-existing faults. The earthquakes in the southeast China coast seismic zone represented by the 1969 Yangjiang earthquake, the historic Nanao

earthquakes in Guangdong Province, and the Zhangzhou earthquakes in Fujian Province, occurred in the passive continental margin, another type of zone of weakness.

The three SCB seismic zones pose significant seismic hazards to metropolitan areas in the SCB. The south Yellow Sea and the downstream Yangtze River seismic zones are the major zones threatened in the Nanjing–Shanghai metropolitan area. The southeast China coastal fold belt seismic zone poses great seismic hazards to the Hong Kong–Shenzhen–Guangzhou metropolitan area. These coastal regions are the economic backbone of China and southeastern Asia. The seismic hazard study in this area is a significant issue that far exceeds pure scientific curiosity. To assess the SCB seismic hazard, it appears that the possible economic loss resulting from a potential earthquake is hard to forecast by groundshaking alone. A more direct way to estimate economic losses, as proposed by CHAN *et al.* (1998), involving use of the gross domestic product (GDP) is worthy of further investigation.

Acknowledgments

I am grateful to Jer-Ming Chiu and Anthony Philpotts for their constructive reviews. I thank Arch Johnston for his stimulation to generate an early edition of this paper. R. Musson of the British Geological Survey kindly provided his compilation of earthquake catalogues in the vicinity of Hong Kong, acquired from historic newspapers. Figure 4 is plotted using the GMT package developed by P. Wessel and W. H. Smith. I am in debt to Kaye Shedlock (USGS), Yong Chen and Ling Chen (China Seismological Bureau), who kindly provided Figure 6a, and Figure 6b, respectively.

Appendix A

Historic Earthquake Events in the South China Block (999 AD–1921)

No.	Year	Month	Day	Longitude	Latitude	Magnitude	Intensity	Location	Iso-intensity	Log(M_0)	M	Remarks
1107	999	10	19	119.9	31.8	5.50	7	Changzhou	y	23.92	5.25	
1116	1045	9	30	112.6	29.9	4.75	6	Jiangling	y	23.12	4.72	
1117	1046	4	18	121.4	36.5	5.50	6	Huanghai	y	23.12	4.72	
1120	1067	11	6	116.5	23.6	6.75	9	Chaozhou	y	25.67	6.41	
1138	1185	6	8	117.6	24.6	6.50	8	Zhangzhou	y	24.77	5.81	
1158	1336	1	12	116.0	31.0	5.50		Taihu	y			
1159	1336	3	6	116.0	30.2	4.75	6	Huangmei	y	23.12	4.72	
1170	1351	8	22	111.8	30.6	4.75		Hubei	y			
	1372	6	1	112.5	23.9	6.20		Guangning				
2001	1372	9	17	113.3	23.1	4.75	6	Guangzhou	y	23.12	4.72	
2003	1407	11		112.6	31.2	5.50	7	Hubei	y	23.92	5.25	
2005	1425	3	7	116.5	31.7	5.75	7	Anhui	y	23.92	5.25	
2009	1445	12	12	117.6	24.5	6.25	8	Fujian	y	24.77	5.81	
2010	1445	12	12	112.6	23.4	4.75	6	Guangdong	y	23.12	4.72	
2015	1469	11	4	112.6	31.2	5.00	7	Hubei	y	23.92	5.25	
2021	1481	3	9				9	Huanghai	y	25.67	6.41	
	1487	6	21	113.9	22.9	4.30		Dongguan				
	1495	7	1	112.2	22.5	4.40		Xinxing				
2041	1505	10	9				9	Donghai	y	25.67	6.41	
	1508	11	3	115.6	23.5	5.10		Jiexi				
	1509	8	13	115.6	23.5	5.10		Jiexi				
2047	1509	3	11	112.4	28.6	4.75	6	Hunan	y	23.12	4.72	
2057	1516	9		118.2	25.1	4.75	6	Fujian	y	23.12	4.72	
	1519	3	11	114.0	22.9	4.50		Dongguan				
2064	1523	8	14	121.7	29.9	5.50	7	Zhejiang	y	23.92	5.25	
2066	1524	4	5	110.5	19.2	5.00	6	Hainan	y	23.12	4.72	
2073	1535	1		117.5	30.7	4.75	6	Anhui	y	23.12	4.72	
2074	1535	5		116.4	25.8	5.00	6	Fujian	y	23.12	4.72	
2077	1537	5	13	117.6	33.6	5.50	7	Anhui	y	23.92	5.25	
2078	1538	10		118.4	24.7	4.75	6	Fujian	y	23.12	4.72	

2090	1558	6	26	111.5	23.4	5.50	7	Guangdong	y	23.92	5.25	
2096	1562			116.0	25.8	5.00	6	Jiangxi	y	23.12	4.72	
2107	1571	5	26	113.5	23.8	5.00	6	Guangdong	y	23.12	4.72	
2111	1574	8	19	119.5	26.2	5.50	7	Fujian	y	23.92	5.25	
2112	1574			119.1	27.6	5.50	7	Zhejiang	y	23.92	5.25	
2120	1584	3	17	115.7	30.8	5.50	7	Hubei	y	23.92	5.25	
2121	1585	3	6	117.7	31.2	5.50	7	Anhui	y	23.92	5.25	
	1589			110.5	24.8	4.50		Yangshou				Musson
2134	1596	10		118.8	25.0	4.75	6	Fujian	y	23.12	4.72	
2139	1600	9	29	117.1	23.5	7.00	9	NanAo	y	25.67	6.41	
2142	1603	5	30	112.6	31.2	5.00	6	Hubei	y	23.12	4.72	
2144	1604	12	29	119.5	25.0	8.00		Quanzhou	y			
2145	1605	7	13	110.5	19.9	7.50	10	Haikou	y	26.61	7.04	
	1605	12	15	110.5	19.9	6.50	8	Haikou		24.77	5.81	Musson
2152	1611	9	9	111.8	21.5	6.00	8	Yangjiang	y	24.77	5.81	Musson
2155	1615	3	1	120.9	32.0	5.00	6	Jiangsu	y	23.12	4.72	
2162	1618			110.1	20.0	5.00	6	Hainan	y	23.12	4.72	
2167	1621			120.7	31.0	5.00	6	Jiangsu	y	23.12	4.72	
2173	1624	2	10	119.5	32.4	6.00	7	Yangzhou	y	23.92	5.25	
2180	1624	9	1	121.5	31.2	5.00	6	Shanghai	y	23.12	4.72	
2184	1626	10	8	109.7	26.9	5.00	6	Hunan	y	23.12	4.72	
2190	1630	2	4	119.2	31.9	4.75	6	Jiangsu	y	23.12	4.72	
2191	1630	Summer		113.5	30.7	5.00	6	Hubei	y	23.12	4.72	
2192	1630	10	14	113.2	30.2	5.00	6	Hubei	y	23.12	4.72	
2194	1631	8	14	111.7	29.3	6.50	8	Hunan	y	24.77	5.81	
2196	1631	9	1	110.2	28.3	5.00	6	Hunan	y	23.12	4.72	
2197	1631	9		105.2	25.8	4.75	6	Guizhou	y	23.12	4.72	
2199	1632			109.7	32.4	5.00	6	Hubei	y	23.12	4.72	
2202	1634	3	30	115.2	30.7	5.50	7	Hubei	y	23.92	5.25	
2209	1640	9		114.9	30.4	5.00	6	Hubei	y	23.12	4.72	
2211	1641	11	26	116.5	23.6	5.75	7	Guangdong	y	23.92	5.25	
2214	1642			118.5	33.0	5.00	6	Jiangsu	y	23.12	4.72	
2216	1644	2	8	117.5	32.9	5.50	7	Anhui	y	23.92	5.25	
3002	1651	2	16	116.6	26.3	5.50	6	Fujian	y	23.12	4.72	
3003	1652	2	10	116.3	31.4	5.50	6	Anhui	y	23.12	4.72	
3004	1652	3	23	116.5	31.5	6.00	8	Anhui	y	24.77	5.81	

Appendix A Continued

No.	Year	Month	Day	Longitude	Latitude	Magnitude	Intensity	Location	Iso-intensity	Log(M_0)	M	Remarks
3007	1653	8	12	110.2	21.7	4.75	5.5	Guangdong	n	22.74	4.46	
3012	1656	3		112.8	22.6	4.75	6	Guangdong	n	23.12	4.72	
3017	1662			120.1	33.4	4.75	6	Jiangsu	n	23.12	4.72	
3022	1665	9	19	111.6	22.7	5.00	6	Guangdong	y	23.12	4.72	
3027	1673	3	29	117.3	31.8	5.00	6	Anhui	n	23.12	4.72	
3033	1676	6	11	119.5	32.4	4.75	6	Yangzhou	n	23.12	4.72	
3037	1678	5	26	121.0	30.5	4.75	6	Zhejiang	n	23.12	4.72	
3041	1679	12	26	119.5	31.4	5.50	7	Jiangsu	n	23.92	5.25	
3044	1683	10	10	113.0	23.1	5.00	6	Guangzhou	y	23.12	4.72	
3050	1693	4	25	115.3	23.0	5.00	6	Guangdong	n	23.12	4.72	
3060	1710	4	16	111.3	27.7	5.00	6	Hunan	y	23.12	4.72	
3076	1731	11	0	121.0	31.3	5.00	6	Jiangsu	y	23.12	4.72	
3090	1742	0	0	110.8	32.1	5.00	6	Hubei	n	23.12	4.72	
3091	1743	6	30	118.4	30.7	5.00	6	Anhui	y	23.12	4.72	
3099	1749	2	28	112.0	22.9	5.00	6	Guangdong	y	23.12	4.72	
3112	1764	6	27	122.0	32.5	6.00		Huanghai	y			
3123	1782	4	30	111.7	26.2	5.00	6	Hunan	y	23.12	4.72	
3134	1791	4	8	117.5	23.8	5.50	7	Fujian	y	23.92	5.25	
3146	1804	Winter	0	115.6	24.9	5.00	6	Jiangxi	n	23.12	4.72	
3149	1806	1	11	115.7	25.3	6.00	8	Jiangxi	y	24.77	5.81	
3155	1813	10	17	120.7	28.0	4.75	5.5	Zhejiang	n	22.74	4.46	
	1817	1	27	113.6	22.3	4.50	5	Macao		22.38	4.22	Musson
	1824	8	14	112.9	23.1	4.80		Sanshui				Musson
3173	1825	10	0	118.9	25.9	4.75	6	Fujian	n	23.12	4.72	
3177	1829	11	18	117.9	33.2	5.50	7	Anhui	y	23.92	5.25	
3180	1831	9	28	116.9	32.9	6.25	8	Anhui	y	24.77	5.81	
3182	1832	1	0	117.0	24.3	5.00	6	Fujian	y	23.12	4.72	
3197	1846	8	4	123.0	32.5	7.00		Huanghai	y			
3203	1852	12	16	122.0	33.5	7.00		Huanghai	y			
3204	1853	2	8	111.7	24.9	4.75	6	Hunan	n	23.12	4.72	
3205	1853	4	14	122.5	33.0	7.00		Huanghai	y			
	1854	9	28	113.6	22.7	4.60	5	Dongguan		22.38	4.22	Musson

3208	1855	Fall	0	108.2	29.3	4.75	6	Sichuan	n	23.12	4.72	
3210	1856	1	4	119.9	30.1	5.00	6	Zhejiang	y	23.12	4.72	
3212	1856	6	10	108.8	29.7	6.25	8	Hubei	y	24.77	5.81	
	1857	1	29	110.3	22.7	4.00	5	Beilu		22.38	4.22	Musson
3220	1863	8	30	114.2	29.1	5.00	6	Jiangxi	y	23.12	4.72	
3222	1866	9	21	119.6	28.6	4.75	6	Zhejiang	n	23.12	4.72	
3223	1867	9		120.5	30.4	4.75	6	Zhejiang	n	23.12	4.72	
3225	1868	10	30	117.8	32.4	5.50	7	Anhui	y	23.92	5.25	
3230	1874	6	23	115.3	23.0	5.00	6	Guangdong	y	23.12	4.72	
3231	1875	6	8	106.3	25.2	6.00		Guizhou				
3237	1878	11	23			6.50		Nanhai	y			
3239	1879	4	4			6.50		Huanghai	y			
3258	1887	4	8	116.8	24.0	5.00	6	Guangdong	y	23.12	4.72	
3261	1887	0	0	111.1	32.4	5.50	7	Hubei	n	23.92	5.25	
3269	1890	8	29	110.5	22.0	6.00		Guangdong	y			
3276	1892	7	28	110.5	19.8	5.00	6	Hainan	y	23.12	4.72	
3281	1893	11	26	107.8	22.8	5.00	6	Guangxi	n	23.12	4.72	
	1894	8	10	116.7	23.4	6.50	7	Shantou		23.92	5.25	Musson
	1894	8	10	116.7	23.4	6.00		Shantou				Musson
3286	1895	8	30	116.4	23.5	6.00	8	Guangdong	y	24.77	5.81	
3296	1899	11	28	109.5	23.3	5.00	6	Guangxi	y	23.12	4.72	
3307	1905	8	12	113.6	22.2	5.00	6	Aomen	y	23.12	4.72	
3312	1906	3	28	118.8	24.5	6.50		Fujian	y			
3314	1906	8	16	111.7	29.1	5.00	6	Hunan	n	23.12	4.72	
3316	1907	10	15	118.6	24.9	5.00	6	Fujian	y	23.12	4.72	
3323	1909	8	11	112.5	23.1	4.75	6	Guangdong	n	23.12	4.72	
3325	1910	1	8	122.0	35.0	6.75		Huanghai	y			
3332	1911	5	15	115.5	22.5	6.00		Guangdong	y			
	1917	1	27	117.0	24.0	6.00		Nanao				Musson
	1918	2	13	117.2	23.5	7.40	10	Nanao		26.61	7.04	Musson
	1921	3	19	116.5	24.0	6.00		Nanao				Musson

Notes:
Column 1: The number is arranged by the volume number of the AHEC plus the event number in that volume.
Column 10: Indication of the iso-intensity map is available in the AHEC.
Column 11: The seismic moment calculated by using JOHNSTON's (1996b) approach.
Column 12: The calculated moment magnitude (HANKS and KANAMORI, 1979).
Column 13: Indication of event ifrom MUSSON (1991, 1995).

REFERENCES

BRANTLEY, B. J., and CHUNG, W.-Y. (1991), *Body-wave Waveform Constraint on the Source Parameters of the Yangjiang, China, Earthquakes of July 25, 1969: A Devastating Earthquake in a Stable Continental Region*, Pure appl. geophys. *135*, 529–543.

CAMPBELL, D. A. (1978), *Investigation of the Stress-concentration Mechanism for Intraplate Earthquakes*, Geophys. Res. Lett. *5*, 477–479.

CHAN, L. S., CHEN, Y., CHEN, Q., CHEN, L., LIU, J., and DONG, W. (1998), *Assessment of Global Seismic Loss Based on Macroeconomic Indicators*, Natural Hazards *17*, 269–283.

CHUNG, W.-Y., and BRANTLEY, B. J. (1989), *The 1984 Southern Yellow Sea Earthquake of Eastern China: Source Properties and Seismotectonic Implications for a Stable Continental Area*, Bull. Seismol. Soc. Am. *79*, 1863–1882.

CHUNG, W.-Y., WEI, B.-Z., and BRANTLEY, B. J. (1995), *Faulting Mechanisms of the Liyang, China Earthquakes of 1974 and 1979 from Regional and Teleseismic Waveforms – Evidence of Tectonic Inversion under a Fault-bounded Basin*, Bull. Seismol. Soc. Am. *85*, 560–570.

CORNELL, C. A. (1968), *Engineering Seismic Risk Analysis*, Bull. Seismol. Soc. Am. *58*, 1583–1606.

DING, G., *Lithospheric Dynamics of China – Explanatory Notes for the Lithospheric Dynamics Atlas of China* (Seismological Press, Beijing 1991).

GIARDINI, D., GRÜNTHAL, G., SHEDLOCK, K., and ZHANG, P. (1999), *The GSHAP Global Seismic Hazard Map*, Annali Geofis. *42*, 1225–1230.

HANKS, T., and KANAMORI, H. (1979), *A Moment Magnitude Scale*, J. Geophys. Res. *84*, 2348–2350.

INSTITUTE OF GEOPHYSICS and INSTITUTE OF CHINESE HISTORICAL GEOGRAPHY, *Atlas of the Historical Earthquakes in China, Ancient to Yuan Dynasty Period* (China Cartographic Publishing House, Beijing 1990).

INSTITUTE OF GEOPHYSICS and INSTITUTE OF CHINESE HISTORICAL GEOGRAPHY, *Atlas of the Historical Earthquakes in China, the Ming Dynasty Period* (China Cartographic Publishing House, Beijing 1990).

INSTITUTE OF GEOPHYSICS and INSTITUTE OF CHINESE HISTORICAL GEOGRAPHY, *Atlas of the Historical Earthquakes in China, the Qing Dynasty Period* (China Cartographic Publishing House, Beijing 1990).

JEAGER, J. C., and COOK, N. G. W., *Fundamentals of Rock Mechanics* (Chapman and Hall, London 1979).

JOHNSTON, A. C. (1996a), *Seismic Moment Assessment of Earthquakes in Stable Continental Regions – I. Instrumental Seismicity*, Geophys. J. Int. *124*, 381–414.

JOHNSTON, A. C. (1996b), *Seismic Moment Assessment of Earthquakes in Stable Continental Regions – II. Historical Seismicity*, Geophys. J. Int. *125*, 639–678.

JOHNSTON, A. C. (1996c), *Seismic Moment Assessment of Earthquakes in Stable Continental Regions – III. New Madrid 1811–1812, Charleston 1886 and Lisbon 1755*, Geophys. J. Int. *126*, 314–344.

JOHNSTON, A. C., and KANTER, L. (1990), *Earthquakes in Stable Continental Crust*, Scientific American, 68–75, March issue.

JUAN, V. C. (1986), *Thermal-tectonic Evolution of the Yellow Sea and East China Sea: Implication for Transformation of Continental to Oceanic Crust and Marginal Basin Formation*, Tectonophysics *125*, 231–244.

KANTER, L., *Tectonic interpretation of stable continental crust*. In *The Earthquakes of Stable Continental Regions: Assessment of Large Earthquake Potential* (ed. Schneider, J., EPRI Report TR-102261) (Electric Power Research Institute, Palo Alto, CA. 1994), pp. 4-1–4-103.

LI, S., and MOONEY, W. D. (1997), *Crustal Structure of China from Deep Seismic Sounding Profiles*, EOS Trans. Am. Geophys. Union *78*, 46, Suppl., 470.

LI, Z.-X. (1994), *Collision between the North and South China Blocks: A Crustal-detachment Model for Suturing in the Region East of the Tanlu Fault*, Geology *22*, 739–742.

LIU, L., *Continental Seismotectonics: Stress, Strain, and Strength*, Ph.D. Thesis, (Stanford University, Stanford, 1993).

LIU, L., LINDE, A. T., SACKS, I. S., and HE, S. (1996), *Fault-block System and Deformation in Northern China*, Pure appl. Geophys. *146*, 717–740.

LIU, L., and ZOBACK, M. D. (1997), *Intraplate Deformation in the New Madrid Seismic Zone*, Tectonics *16*, 585–595.

MA, X., *Lithospheric Dynamics Atlas of China* (China Cartographic Publishing House, Beijing 1989).

MITCHELL, B. J., PAN, Y., CHEN, D., and XIE, J. (1993), *Q and Crustal Evolution in Stable Continental Regions*, Seismol. Res. Lett. *64*, 262.

MUELLER, B., WEHRLE, V., and FUCHS, K., *The 1997 Release of the World Stress Map* (available on-line at http://www-wsm.physik.uni-karlsruhe.de/pub/Rel97/wsm97.html) (1997).

MUSSON, R. M., *A Provisional Earthquake Catalogue for the Hong Kong Region* (British Geological Survey Technical Report WL/91/39, 1991).

MUSSON, R. M. (1995), *Historical Seismicity of South China from European Sources*: *Example of the Hong Kong Newspaper Press*, Acta Seismologica Sinica *8*, 487–490.

NUTTLI, O. W. (1973), *The Mississippi Valley Earthquakes of 1811 and 1812*: *Intensities*, *Ground motion and Magnitudes*, Bull. Seismol. Soc. Am. *63*, 227–248.

POLLACK, H. N., HURTER, S. J., and JOHNSON, J. R. (1993), *Heat Flow from the Earth's Interior*: *Analysis of the Global Data Set*, Rev. Geophys. *31*(3), 267–280.

ROYDEN, L., BURCHFIEL, B. C., KING, R., WANG, E., CHEN, Z., SHEN, F., and LIU, Y. (1997), *Surface Deformation and Lower Crustal Flow in Eastern Tibet*, Science *276*, 788–790.

SEEBER, L., and ARMBRUSTER, J. G., *Earthquakes and pre-existing structure in stable continental regions* (Abstract of the AGU Chapman Conference on Stable Continental Region (SCR) Earthquakes, pp. 38–39, Hyderabad, India, January 25–29, 1998).

SEGUIN, M. K., and ZHAI, Y. (1995), *Paleomagnetic Constraints on the Convergence of the Sino–Korean and Yangtze Blocks*, *China*, Acta Geophysica Sinica *38*, 34–45.

STATE STATISTICAL BUREAU OF CHINA, *1998 China Statistical Yearbook* (1999).

SYKES, L. R. (1978), *Intraplate Seismicity*, *Reactivation of Pre-existing Zones of Weakness*, *Alkaline Magmatism*, *and Other Tectonism Postdating Continental Fragmentation*, Rev. Geophys. *16*, 621–688.

TALWANI, P. (1999), *Fault Geometry and Earthquakes in Continental Interiors*, Tectonophysics *305*, 371–379.

WANG, L., LI, C., SHI, Y., and WANG, Y. (1995), *Distribution of Geo-temperature and Terrestrial Heat Flow Density in Lower Yangtze Area*, Acta Geophysica Sinica *38*, 469–476.

WESNOUSKY, S. G., and SCHOLZ, C. H. (1980), *The Craton*: *Its Effect on the Distribution of Seismicity and Stress in North America*, Earth Planet. Sci. Lett. *48*, 348–355.

XIE, D., MAO, J., PENG, W., ZHAO, Y., and JIANG, Y. (1997), *The Rock Strata of South China and Continental Dynamics*, Acta Geophysica Sinica *40*, Suppl., 153–163.

YANG, W., GUO, T., LU, Y., ZHENG, J., SU, J., and MA, X. (1984), *Opening and Closing in the Tectonic Evolution of China*, Earth Sci. *3*, 39–56.

ZENG, R., SUN, W., MAO, T., LIN, Z., HU, H., and CHEN, G. (1995), *The Depth of Moho in the Mainland China*, Acta Seismologica Sinica *8*, 399–404.

ZHANG, P., YANG, Z., GUPTA, H. K., BHATIA, S. C., and SHEDLOCK, K. M. (1999), *Global Seismic Hazard Assessment Program (GSHAP) in Continental Asia*, Annali di Geofisica *42*, 1167–1190.

ZOBACK, M. L. (1992), *First- and Second-order Patterns of Stress in the Lithosphere: World Stress Map Project*, J. Geophys. Res. *97*, 11703–11728.

(Received August 8, 2000, accepted November 15, 2000)